Soils and Rocks
An International Journal of Geotechnical and Geoenvironmental Engineering
www.soilsandrocks.com
ISSN 1980-9743
ISSN-e 2675-5475

A coupled hydromechanical model including fracture propagation along the dam foundation interface for gravity dam's stability assessment

Maria Luísa Braga Farinha[1#], Nuno Monteiro Azevedo[1], Sérgio Oliveira[1]

Article

Keywords
Gravity dam
Hydromechanical coupled model
Fracture propagation
Safety assessment

Abstract

Most gravity dam failures occur due to sliding along the dam/foundation interface, rock mass discontinuities, or rock mass layers of lower strength. The possibility of sliding of a dam is usually evaluated based on simplified limit equilibrium techniques. In this study an explicit time-stepping small displacement algorithm, Parmac2D-Fflow, is used to assess the safety of gravity dams. This algorithm is based on a discrete representation of discontinuities, simulates the hydromechanical interaction, and considers softening constitutive laws that are closer to the actual behaviour of the dam/foundation interface. Seepage flow along the dam/foundation interface is only allowed to occur after contact failure, making it possible to model a coupled propagation failure along the dam/foundation interface due to a hypothetical dam overtopping scenario. For two gravity dams with different heights, the numerical results predicted with a coupled/fracture propagation model are compared with those obtained with a coupled/fully fractured model and with an uncoupled analysis. The results presented highlight the relevance of considering a coupled hydro-mechanical model for dam safety analysis and show that with a coupled-fracture propagation model slightly higher safety factors are predicted.

1. Introduction

Concrete gravity dams are built on rock foundations, and stability analysis involves identifying potential sliding block mechanisms that could lead to failure. The behaviour of the rock mass is primarily governed by sliding either along the dam/concrete interface or along weak, sub-horizontal layers in the foundation, near the base of the dam (Azevedo et al., 2021; Farinha et al., 2022). The geological and geotechnical characteristics of the foundation area play a crucial role in the dam's performance, and seepage studies are commonly conducted to assess the dam's global stability (Santos et al., 2023). These studies are sometimes complemented with sensitivity analysis of dam model outputs (He et al., 2022; Li, 2021).

The hydromechanical behaviour of fractured rock masses is critical and must be carefully considered, with the behaviour of discontinuities represented by realistic constitutive models (Farinha et al., 2022; Zhou et al., 2022). For concrete dam foundations, discontinuum models that simulate hydromechanical interactions offer a valuable approach for assessing dam stability. These models account for actual shear displacements, the aperture of discontinuities, and the water pressure distribution within the foundation. Regarding the failure mechanism that involves sliding and the possibility of crack formation and propagation along the dam base, studies have been performed to investigate the interface properties and associated failure processes between dam concrete and rock (Dong et al., 2016, 2024; Li et al., 2022; Tian et al., 2015) and its effect on the stability of dams (Krounis et al., 2015).

This study uses a coupled hydromechanical model to evaluate the stability of gravity dams, accounting for the opening and closing behaviour of discontinuities, as well as the influence of water pressure within the foundation joints and along the dam/foundation interface. The model incorporates interface elements that simulate a reduction in cohesion and tensile strength at both concrete/concrete and concrete/rock interfaces. Stability assessments are performed on two gravity dams of varying heights. The safety factors against sliding are calculated using a gradual load amplification approach, applying a softening behaviour to joint elements that simulate the discontinuities (concrete/concrete and concrete/rock) (Azevedo et al., 2010) and (Azevedo & Lemos, 2022). Two different assumptions for the behaviour of the foundation rock mass are considered: either linear elastic or brittle failure. A critical evaluation of the results is provided in the context of sliding safety.

#Corresponding author. E-mail address: lbraga@lnec.pt
[1]Laboratório Nacional de Engenharia Civil, Departamento de Barragens de Betão, Lisboa, Portugal.

Submitted on January 31, 2025; Final Acceptance on September 19, 2025; Discussion open until February 28, 2026.
Editor: Renato P. Cunha
https://doi.org/10.28927/SR.2025.002125

2. Numerical modelling approach

2.1. Coupled hydromechanical model

This study was carried out with *Parmac2D-Fflow* (Farinha et al., 2017; Azevedo et al., 2021), which allows fully coupled hydromechanical analysis. The mechanical domain is divided into blocks, which are internally divided into a mesh of plane triangular elements to simulate their deformability. The interaction between these deformable blocks, which simulate both the dam and the foundation, is done using joint finite elements under a small displacement hypothesis (Figure 1a). The hydraulic model is perfectly superimposed on the mechanical model and thus for each joint element (JE) there is a corresponding seepage channel (SC), as shown in Figure 1b), with a hydraulic node (HN) at each end of the seepage channel.

2.2. Bilinear softening contact model

A bilinear softening constitutive law, in the normal and shear directions, was adopted to represent the behaviour of both concrete/concrete and concrete/rock discontinuities (Figure 2). This model has been applied to particle modelling of rock and concrete fracture studies (Azevedo et al., 2010; Azevedo & Lemos, 2022). From the moment the maximum strength values (tensile and cohesion) are reached, the maximum strength tensile force and/or the maximum cohesion are reduced based on the damage value, which varies between 0 (no damage) and 1 (contact considered cracked, only working in pure friction). The strength parameters of this contact model are: the maximum tensile strength (σ_t), the maximum cohesion stress (C_{max}), the friction coefficient (μ_c), the fracture energy in mode I (G_I) and the fracture energy in mode II (G_{II}).

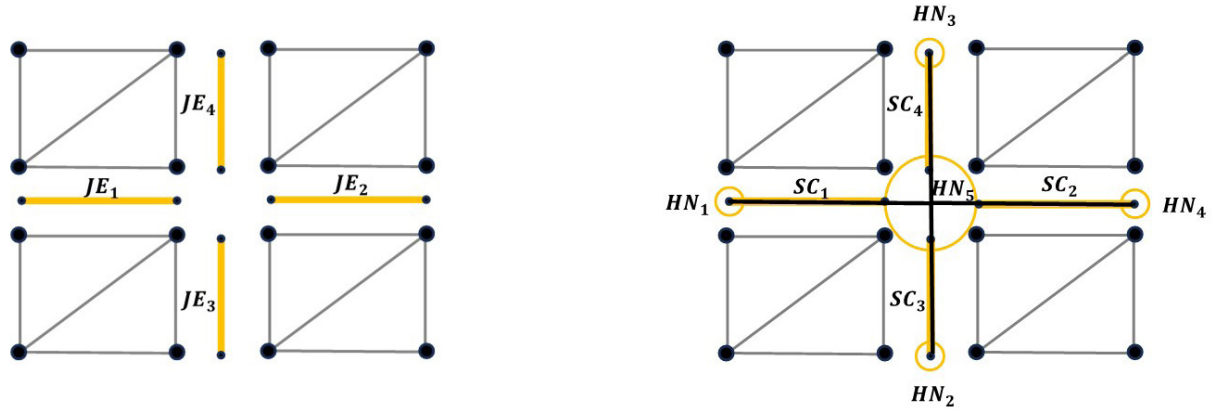

Figure 1. Hydraulic and mechanical models superimposed: (a) Mechanical model joint elements (JE); (b) hydraulic model nodes (HN) and seepage channels (SC).

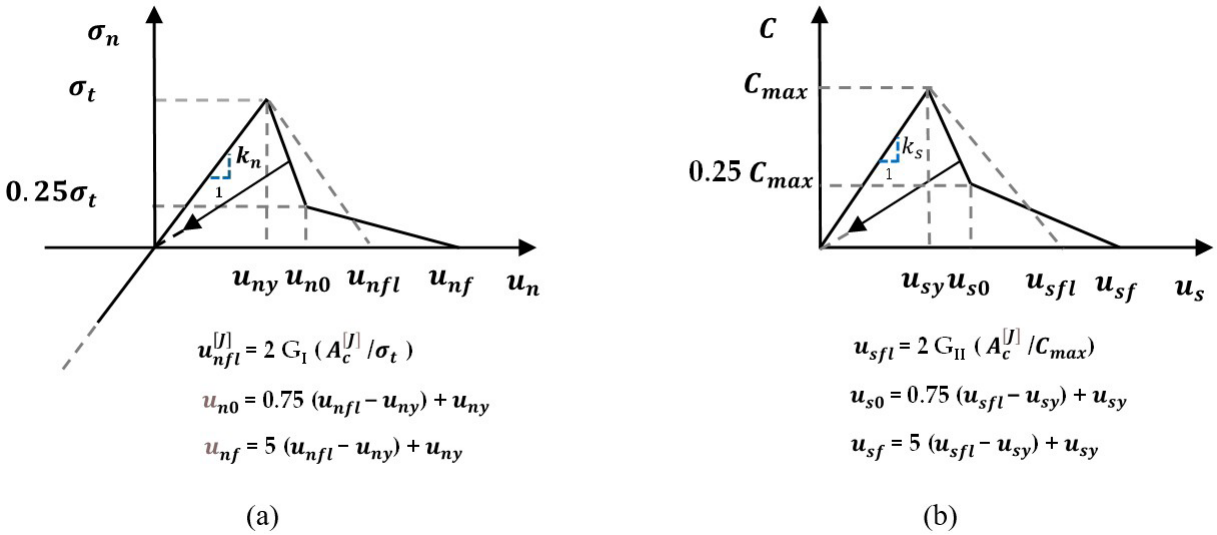

Figure 2. Bilinear vectorial-softening interface model (BL): a) normal direction; and b) shear direction.

3. Stability analysis of gravity dams

3.1. Model description

3.1.1 Geometry and boundary conditions

This study examined four different models, each representing one of two large gravity dams with varying heights (15 m and 30 m), with their foundations on rock masses characterized by two distinct fracture patterns. Figure 3 shows the schematic layout of these models, where all dimensions are expressed in relation to the dam height (H) and the top thickness of the dam (a).

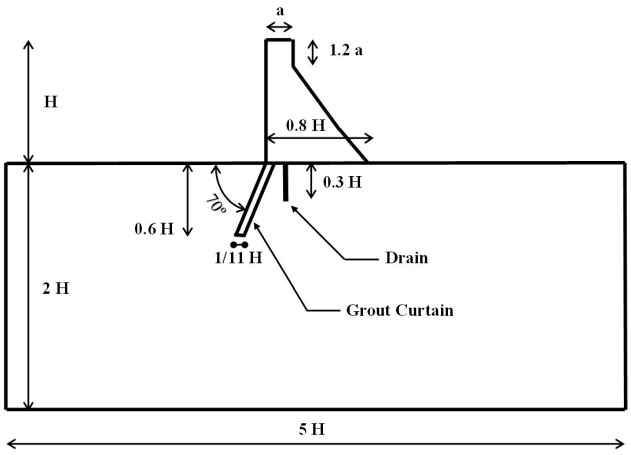

Figure 3. Dam/foundation system model geometry.

As shown in Figure 4, the construction joints within the concrete dam structure were simulated using a set of horizontal discontinuities, with a spacing of 3.0 m, and the foundation rock masses were represented with different sets of discontinuities:

i) The first model, called "reg", includes a set of continuous horizontal discontinuities spaced 5.0 m apart, along with a second set of vertical cross-joints. These vertical joints have an average spacing of 5.0 m perpendicular to the joint traces, with a standard deviation from the mean of 1.0 m.

ii) The second model, called "dip", features two sets of continuous orthogonal discontinuities that make angles of 15º and 105º with the horizontal.

It is important to highlight that in the "dip" model, the alignment, and the continuity of the two sets of flat discontinuities in the foundation promote the development of potential failure mechanisms, particularly the formation of sliding wedges beneath the dam.

In addition to the sets of discontinuities, Figure 4 also shows the internal mesh of both dam and foundation blocks, composed of triangular plane finite elements.

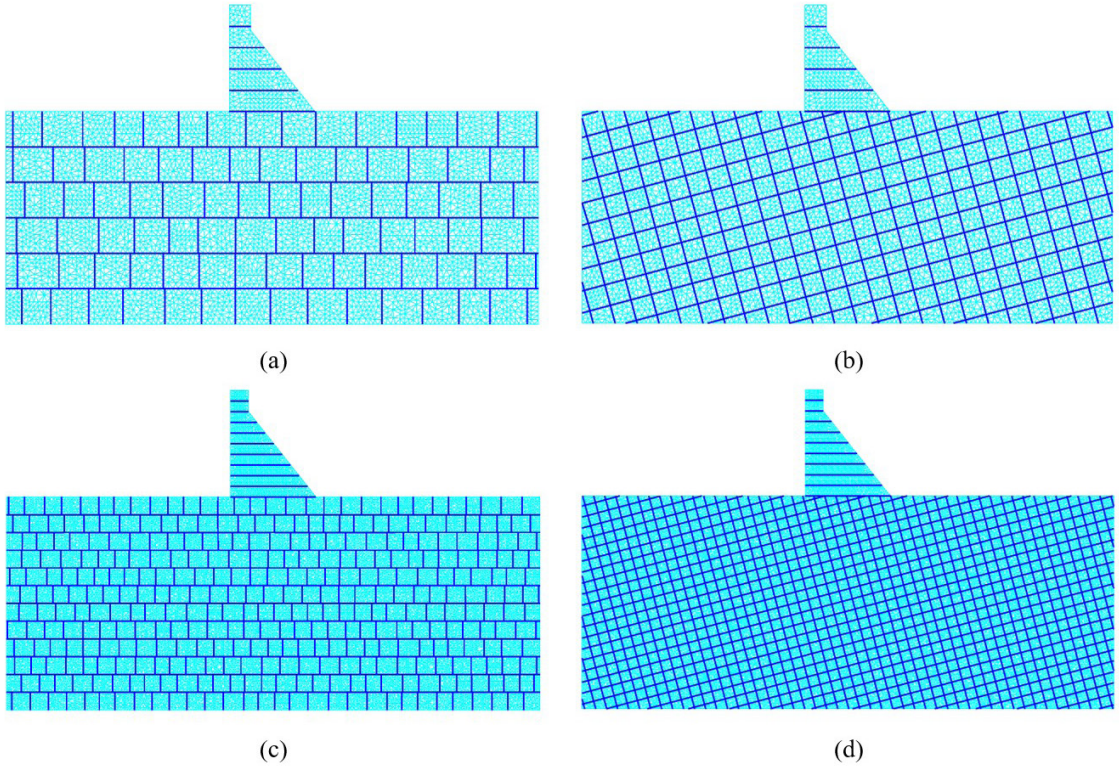

Figure 4. Dam/foundation system discontinuous models: (a) model 15-reg; (b) model 15-dip 15 m high gravity dam; (c) model 30-reg; (d) model 30-dip 30 m high gravity dam. In each block a triangular plane finite element discretization is adopted.

Figure 5 shows the hydraulic part of the models, based on the assumption that water seepage occurs exclusively along the dam/foundation interface and through the network of discontinuities within the foundation.

Table 1 shows the number of mechanical and hydraulic elements included the four different models. It should be mentioned that, for both dam heights, the average edge length of the triangular elements is 0.6 m.

Regarding the mechanical boundary conditions, the bottom of the model was restrained and horizontal displacements on the lateral boundaries were restricted. For the hydraulic boundary conditions, impermeability was assumed at both the base and the sides of the model, and the drainage system was simulated by assigning a water pressure along the drain axis equal to 1/3 of the hydraulic head upstream from the dam.

3.1.2 Material properties

The dam concrete and the foundation rock blocks are modelled with elastic behaviour, with the material properties shown in Table 2 which include Young´s modulus (*E)*, Poisson's coefficient (v), and density (ρ). In the concrete region, joints are assigned a normal stiffness (k_n) of 60.6 GPa/m and a shear stiffness (k_s) of 24.2 GPa/m. For both the dam/foundation interface and the discontinuities within the rock mass, the stiffness values are k_n = 120.8 GPa/m and k_s = 51,5 GPa/m. When non-linear behaviour is considered in the rock mass discontinuities, the model assumes zero cohesion and tensile strength, with a friction angle of 45º.

For the hydraulic apertures of the seepage channels, the following values were used: $a_0 = 1.668\times10^{-4}$ m, $a_{res} = 1/3 \times a_0$ and $a_{max} = 5 \times a_0$ (a_0 is the joint aperture at nominal zero normal stress, a_{res} is the residual aperture and a_{max} is the maximum hydraulic aperture). The permeability of the dam/foundation interface was assumed to be half that of the discontinuities within the foundation. The grout curtain was modelled with a permeability 2.5 times lower than that of the surrounding rock. The construction joints within the dam were treated as impermeable. Table 3 shows the contact model parameters of the adopted contact interface bilinear softening constitutive law.

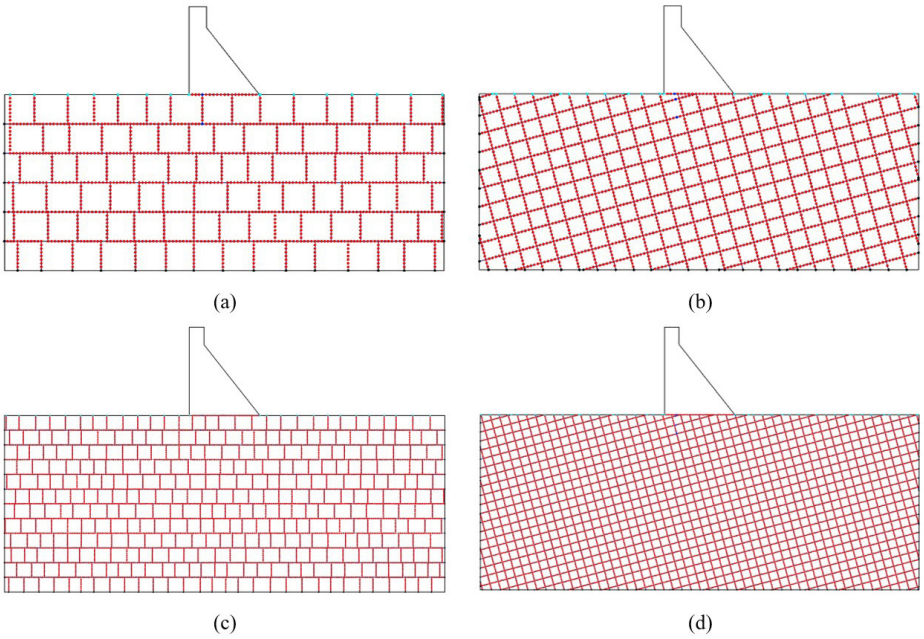

Figure 5. Foundation hydraulic models. Hydraulic head assumed on the rock mass surface upstream and downstream from the dam (light blue dots); hydraulic head assumed at the drainage system (dark blue dots); hydraulic channels (red dots); impervious lateral and bottom model boundaries (black dots): (a) model 15-reg; (b) model 15-dip; (c) Model 30-reg; (d) model 30-dip.

Table 1. Number of different elements in each model.

Model	*a**	*b**	*c**	*d**	*e**
15-reg	6531	9629	1420	1322	1379
15-dip	8063	10058	2550	2299	2509
30-reg	25883	38549	5843	5367	5659
30-dip	31784	40178	10221	9115	10037

**a*: mechanical nodal points; *b*: triangular elements; *c*: joint elements; *d*: hydraulic nodal points; *e*: seepage channels.

Table 2. Material mechanical properties (after Dong et al., 2016).

Material	E	v	ρ
	(GPa)	(-)	(kN/m^3)
Dam concrete	30.3	0.24	2400
Rock mass	64.4	0.20	2700

Table 3. Softening model parameters for the two different discontinuities: concrete/rock and concrete/concrete.

σ_t	G_I	C_{max}	G_{II}	μ_c
(MPa)	(Nm/m2)	(MPa)	(Nm/m^2)	(-)
2.9	250	8.0	2500.0	1.0

σ_t: maximum tensile strength; G_I: fracture energy in mode I; C_{max}: maximum cohesion stress; G_{II}: fracture energy in mode II; μ_c: friction coefficient.

3.2 Stability assessment

The models developed were used to evaluate the sliding safety of the dam/foundation system, considering the possibility of sliding occurring not only at the dam/foundation interface but also within the discontinuities of the foundation rock mass. The analysis was performed in two stages. In the first stage, a hydromechanical calculation was carried out, taking into account the weight of the dam, assuming that the water table was at ground level with an initial in situ horizontal-to-vertical effective stress ratio of 0.5. In the second stage, the hydrostatic pressure was applied at the upstream face of the dam and at the base of the reservoir, under the assumption that all the discontinuities exhibited linear elastic behaviour. This second stage involved a mechanical analysis, followed by a hydromechanical analysis. In cases where non-linear behaviour of the discontinuities was assumed, this was only considered after equilibrium had been reached. Throughout all simulations, the reservoir was assumed to be at the dam crest level.

For each gravity dam the results obtained using a coupled model with fracture propagation were compared to those from a coupled model assuming fully developed fractures, as well as to an uncoupled analysis in which water pressures remained fixed at the values corresponding to the initial equilibrium state (no hydraulic computation was performed in this model). In the coupled simulations, the hydraulic head upstream from the dam was gradually increased given the water height above the dam crest. In the fracture propagation model, seepage along the dam/foundation interface was permitted only after damage had initiated in the corresponding joint elements.

The safety of concrete dams is commonly expressed through a factor of safety, which can be determined either by following a strength reduction of the discontinuities involved in potential failure mechanisms (Farinha et al., 2017) or by increasing the hydrostatic load on the upstream face of the dam (Azevedo et al., 2021; Enzell et al., 2023), the latter being adopted in this work.

Figure 6 shows the hydraulic head contours for the 30-reg model assuming a brittle model for the foundation behaviour, for the case where seepage is considered along the dam foundation interface since the beginning of the hydromechanical analysis and for the case where seepage along the dam/foundation interface is just allowed after damage initiation at each joint element. As shown, at the vicinity of the dam foundation the hydraulic head is slightly different on both calculation hypothesis, but outside this area the hydraulic head distribution is quite similar. On both models the effect of the drainage system on the hydraulic head is clearly visible. Figure 7 shows the distribution of water pressures along the base of the dam obtained for the two seepage assumptions. As shown, at the beginning of the load amplification calculation there is no damage at the dam/foundation interface joint elements (zero pressure), whereas in the scenario where seepage is allowed from the beginning of the calculations the predicted pressure distribution is closer to the bi-linear uplift distribution that is usually assumed in stability design.

Figure 8 and Figure 9 show the horizontal crest displacement during the process of amplification of water pressure for both the 15 m and 30 m high gravity dams. For the four different models the load amplification analysis was carried out assuming three different hypotheses: uncoupled (UCP), coupled (CP) and coupled behaviour with fracture propagation due to water pressure (CP-FP) and two different foundation behaviours: elastic (E) and brittle model (B).

As shown in Figures 8 and 9, for both dam heights, with a fractured foundation following a brittle model a higher crest displacement is predicted when compared with an elastic foundation. In addition, with a brittle foundation the difference in behaviour when load coupling is considered (CP, CP-FP) is more noticeable when compared with the uncoupled models (UCP), where the pressures remained constant and equal to those obtained in the initial equilibrium situation.

For the Model 15-reg the CP hypothesis leads as expected to the lowest water height above the crest. For the Model 15-dip the CP hypothesis also leads to the lowest water height

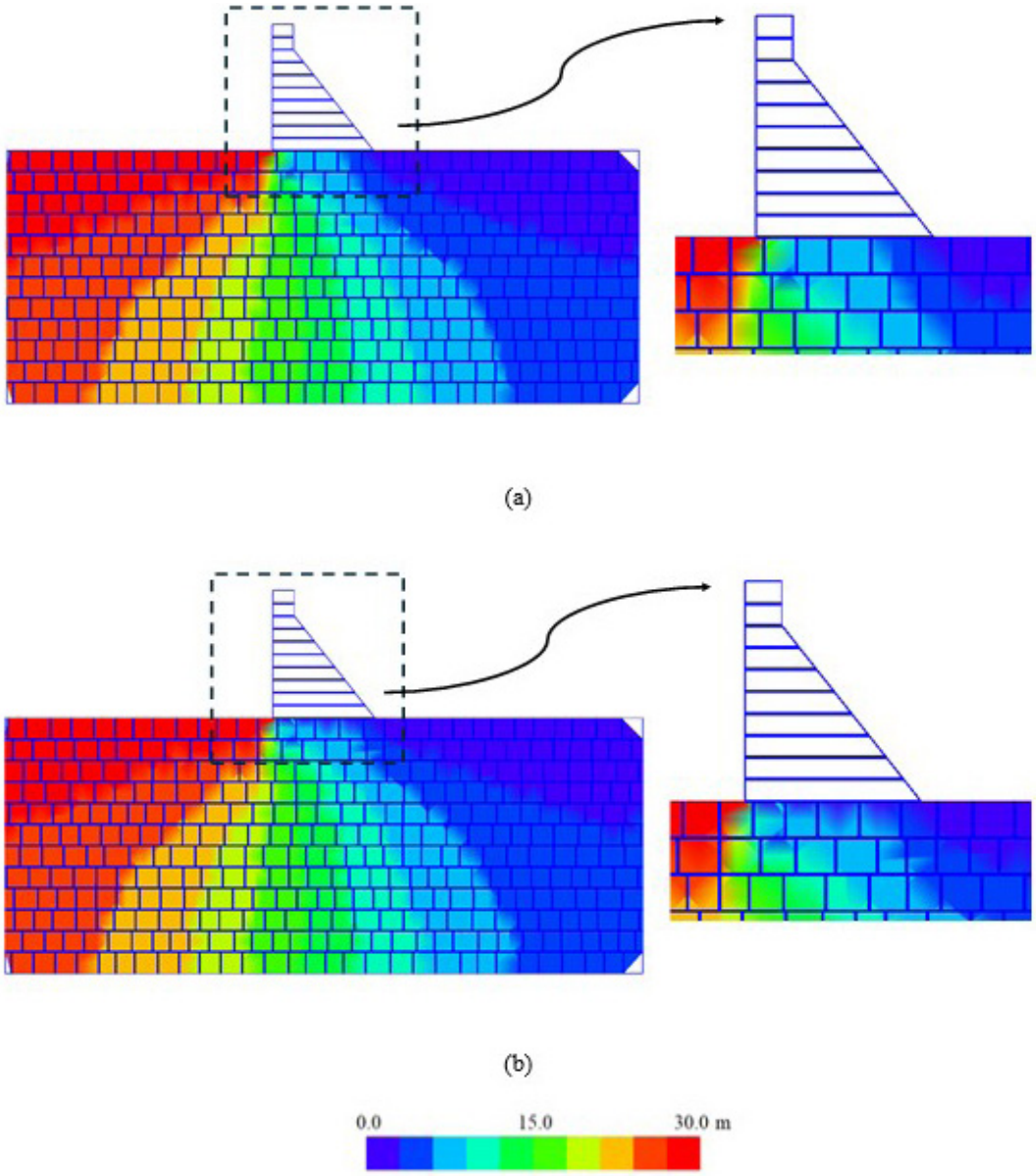

Figure 6. Hydraulic head contours: model 30-reg for a foundation with a brittle model: (a) seepage is considered along the dam foundation since the beginning of the hydromechanical analysis (S); (b) seepage along the dam/foundation interface is just allowed after damage initiation (S-FP).

above the crest, but for a fracture foundation, the predicted water height is similar to the water height predicted with a CP-FP hypothesis. When an elastic behaviour is assumed for the foundation, the CP-FP hypothesis predicts a water level above the crest higher than the value predicted with a UCP approach. When a fractured behaviour is assumed for the foundation, the UCP hypothesis predicts a water level above the crest higher than the value predicted with a CP-FP approach. A similar behaviour is predicted for the 30 m dam height. The main difference occurs in the Model 30-dip for a fractured foundation, where a slightly higher water level above the crest is predicted with the CP model when

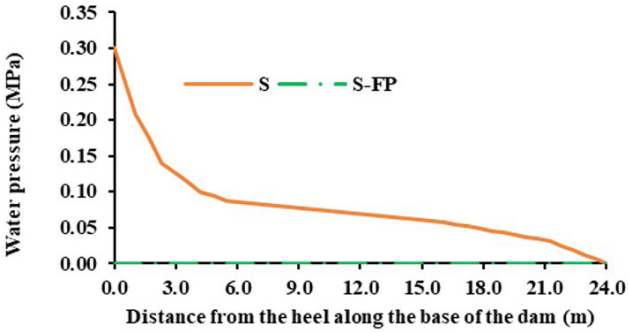

Figure 7. Water pressures along the dam/foundation interface: model 30-reg for a foundation with a brittle model.

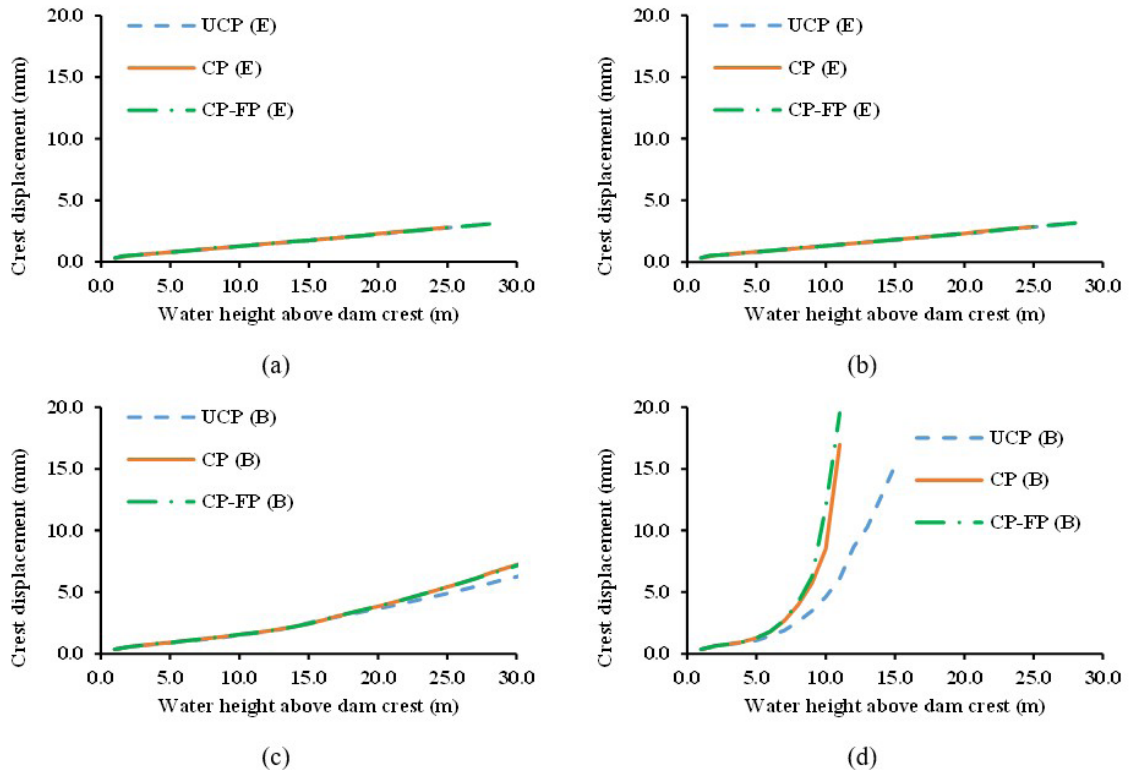

Figure 8. Horizontal crest displacement during the process of amplification of water pressure for: (a) model 15-reg (E); (b) model 15-dip (E), Model 15-reg; (c) model 15-reg (B); (d) model 15-dip (B).

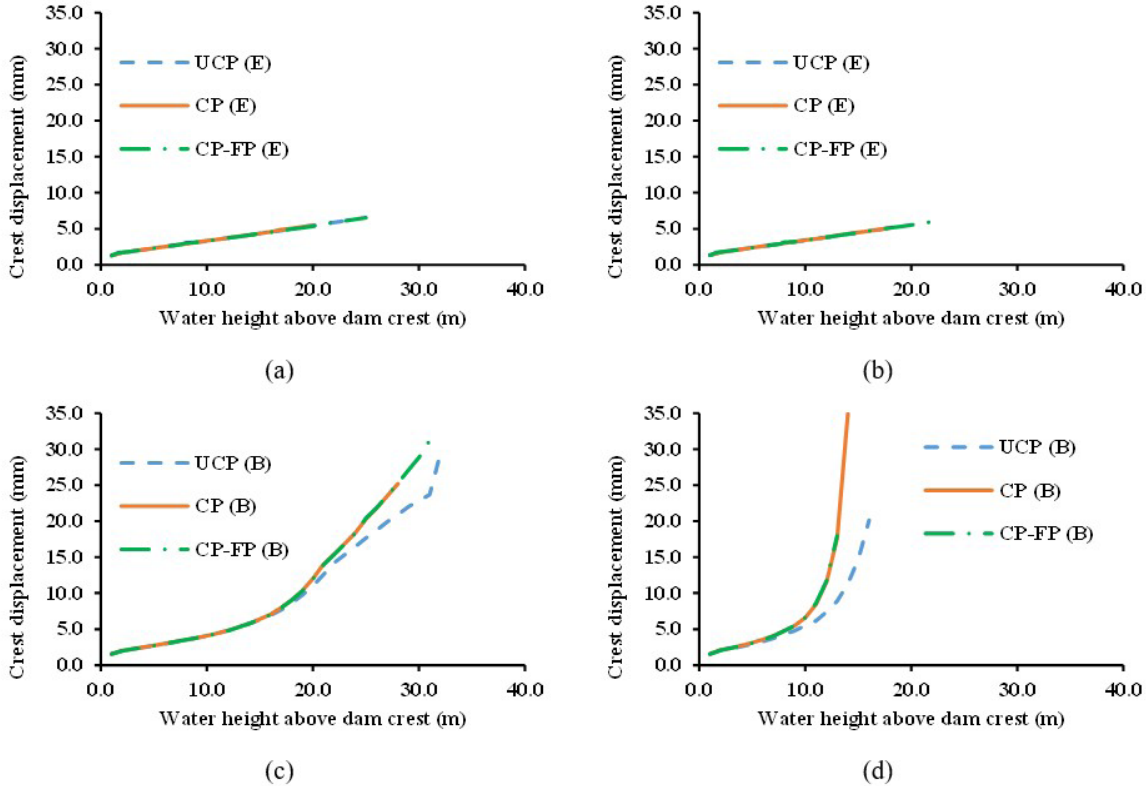

Figure 9. Horizontal crest displacement during the process of amplification of water pressure for: (a) model 30-reg (E); (b) model 30-dip (E), Model 30-reg; (c) model 30-reg (B); (d) Model 30-dip (B).

compared with the water level predicted with the CP-FP hypothesis, this is mainly due to the fact that seepage at the dam/foundation occurs due to damage only at the highest water value which originates additional difficulties to converge to a stable equilibrium position.

Table 4 shows the safety factors calculated for the four different models based on numerical analyses performed under three different assumptions: uncoupled (UCP), coupled (CP) and coupled with water pressure-induced fracture propagation (CP-FP), and two different foundation behaviours: elastic (E) and brittle model (F).

Assuming an elastic foundation model (E) the safety factor obtained with the simplified uncoupled model (UCP) is always higher than that obtained with a coupled model (CP), in which a permeable dam/foundation interface is considered from the beginning of the load amplification process. When using the coupled model that incorporates fracture propagation (CP-FP) along the dam–foundation interface, the resulting safety factors are, as anticipated, higher than those obtained with the standard coupled model (CP) and also exceed those derived from the simplified uncoupled model (UCP).

Assuming a fractured foundation following a brittle model (B) the safety factor calculated with the simplified uncoupled model (UCP) is always the highest. The coupled model that includes fracture propagation (CP-FP) along the dam/foundation interface leads to a higher safety factor compared with the coupled model (CP), which assumes the interface is permeable from the start of the load amplification process, except for model 30-dip.

As expected, for a brittle foundation (B) in which the orientation of the discontinuity sets favours the formation of failure mechanisms (15-dip and 30-dip), the predicted safety factors are, for all analysis assumptions, consistently lower than those obtained for the models with a regular foundation (15-reg and 30-reg).

Overall, the results here presented indicate that with an uncoupled model (UCP) the calculated safety factor may be higher than that obtained with a coupled fracture propagation model (CP-FP). The results presented also show that the coupled model (CP), that considers the dam/foundation interface permeable from the start of the safety factor calculation, leads to a safety factor equal or lower than that predicted with the coupled fracture propagation model (CP-FP), except for model 30-dip.

Figure 10 shows the expected predicted sliding failure mode for the 30 m high dam assuming an elastic foundation for the coupled model taking into account fracture propagation (CP-FP). A similar failure is predicted with the UCP and CP models. For both foundation geometries the failure mode is mostly due to the sliding of the dam at the concrete/rock interface with a less significant rotation about the downstream foot, which is slightly more noticeable at the onset of failure for the coupled approaches (CP, CP-FP).

Table 4. Safety factors: elastic foundation (E) and fractured foundation (F).

Model	15-reg	15-dip	30-reg	30-dip
UCP (E)	4.60	4.73	2.53	2.27
CP (E)	4.33	4.33	2.33	2.20
CP-FP (E)	4.87	4.87	2.67	2.47
UCP (F)	5.80	3.00	3.13	2.07
CP (F)	5.13	2.47	2.87	1.93
CP-FP (F)	5.67	2.47	3.07	1.87

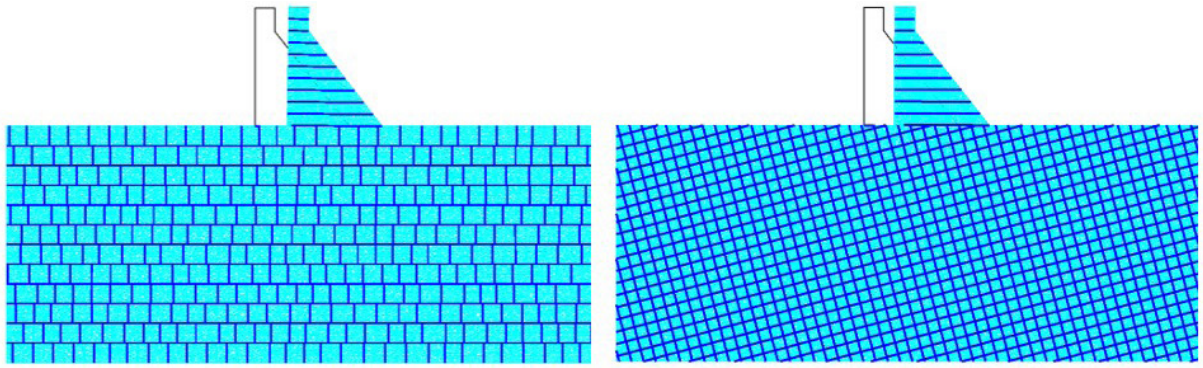

Figure 10. Failure modes for the 30 m high dam with elastic foundation for the maximum load amplification factors: (a) model 30-reg (CP-FP), displacement magnified 2.5 times; (b) model 30-dip (CP-FP), displacement magnified 5.0 times.

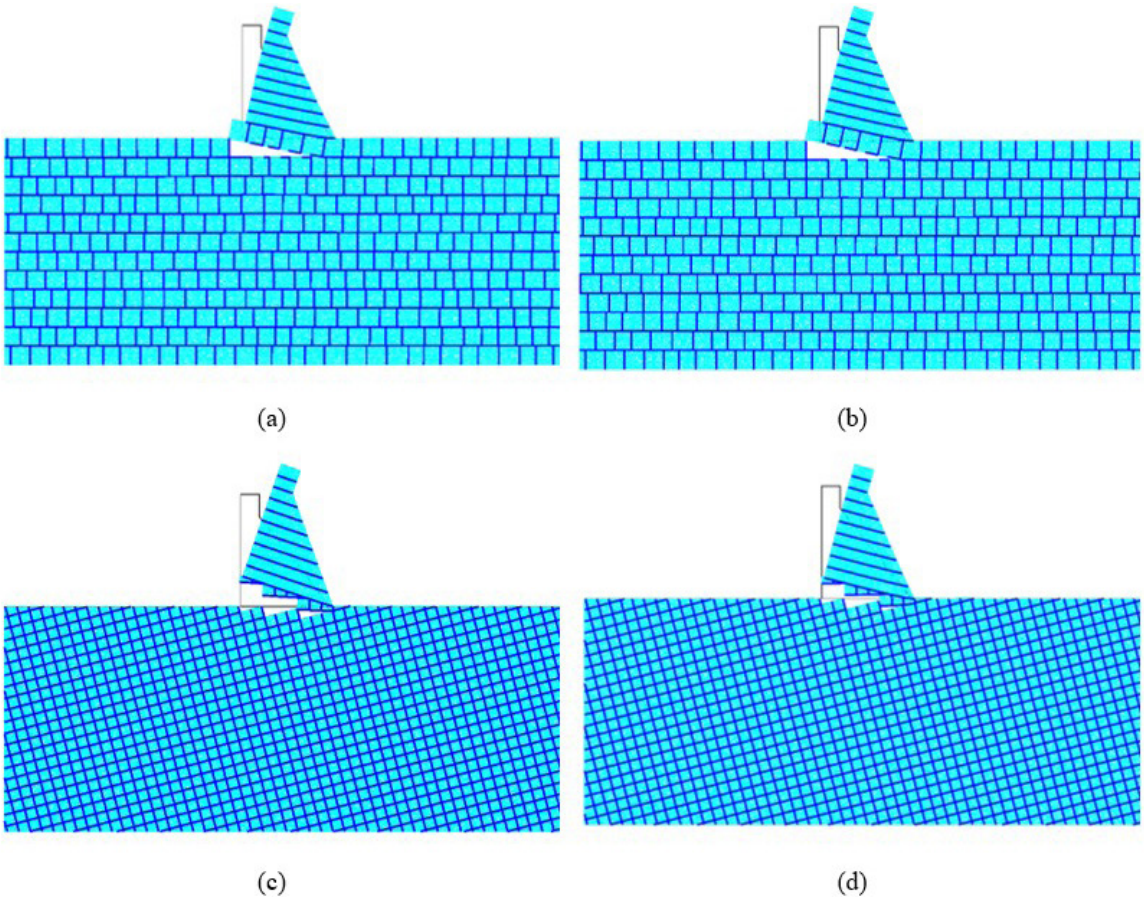

Figure 11. Failure modes for the 30 m high dam with brittle foundation for the maximum load amplification factors: (a) model 30-reg (CP), displacement magnified 300 times; (b) model 30-reg (CP-FP), displacement magnified 350 times; (c) model 30-dip (CP), displacement magnified 75.0 times; (d) model 30-dip (CP-FP), displacement magnified 250 times.

Figure 11 shows the predicted failure modes for a fractured foundation, for the 30 m high dam using both the coupled model (CP) and the coupled model taking into account fracture propagation (CP-FP). Under both hypothesis and dam geometries the predicted failure modes are more complex than the sliding failure mode shown in Figure 10, as the sliding of the dam is accompanied with a more meaningful rotation at the toe of the dam and failure mode involves opening of discontinuities in the foundation rock mass near the heel of the dam.

As shown in Figures 10 and 11, the failure modes obtained, for this set of contact strength parameters, dam heights, and foundation geometries, with the CP and CP-FP approaches are similar. This means that although in the CP-FP approach water seepage only takes place as crack occurs, the fracture propagation influence is not meaningful in the final failure mode.

4. Conclusion

The safety evaluation of gravity dams should follow the proposed framework that considers a load amplification approach using a coupled hydromechanical model, material properties closer to the real material response and foundation geometries and behaviours as close as possible to the reality. Compared to the traditional strength reduction approach, typically used in foundation design, and referenced in current dam safety design guidelines, this strategy yields more realistic safety factors and failure mechanisms. In the context of coupled analyses, assuming an initially impervious dam/foundation interface may offer a more accurate representation of actual conditions. The results presented show that slightly higher safety factors are predicted when fracture propagation is accounted for during the load amplification process.

The outcomes of safety assessments for existing dams under overtopping conditions, whether caused by floods exceeding design expectations or by the effects of climate change, and under seismic loading, can support the establishment of alert thresholds for use in predictive models. The proposed methodology can be adopted to identify and anticipate potential failure scenarios, and additionally it can be used in the development of a comprehensive failure analysis database.

Ongoing research is focused on evaluating the performance of the coupled model with fracture propagation across a wide range of material properties, including those for concrete, rock mass and corresponding interfaces, as well as different material behaviours, including nonlinear behaviour at both the dam and foundation areas, dam geometries and the consideration of a downstream rock wedge that enhance dam stability.

Acknowledgements

The study presented here is part of the research project StepDam: A step forward for the ability to anticipate and prevent failures of concrete dam foundations (Proc. 0403/1102/24145, included in LNEC´s Research and Innovation Plan 2021-2027).

Declaration of interest

The authors have no conflicts of interest to declare. All co-authors have observed and affirmed the contents of the paper and there is no financial interest to report.

Authors' contributions

Maria Luísa Braga Farinha: conceptualization, methodology, validation, supervision, project administration, writing – original draft, writing – review & editing. Nuno Monteiro Azevedo: conceptualization, software, methodology, validation, supervision, project administration, writing – original draft, writing – review & editing. Sérgio Oliveira: conceptualization, validation, software, writing – review & editing.

Data availability

The datasets generated analyzed in the course of the current study are available from the corresponding author upon request.

Declaration of use of generative artificial intelligence

This work was prepared without the assistance of any generative artificial intelligence (GenAI) tools or services. All aspects of the manuscript were developed solely by the authors, who take full responsibility for the content of this publication.

List of symbols and abbreviations

a_0	Joint aperture at nominal zero normal stress
a_{max}	Maximum hydraulic aperture
a_{res}	Residual aperture
k_n	Joint normal stiffness
k_s	Joint shear stiffness
B	Brittle model
C_{max}	Maximum cohesion stress
CP	Coupled model
CP-FP	Coupled model with fracture propagation
E	Elastic model
E	Young's modulus
G_I	Fracture energy in mode I
G_{II}	Fracture energy in mode II
H	Height of the dam
HN	Hydraulic node
JE	Joint Element
SC	Seepage channel
UCP	Uncoupled model
μ_c	Friction coefficient
ν	Poisson's ratio
ρ	Density
σ_t	Maximum tensile strength

References

Azevedo, N.M., Farinha, M.L.B., Sá, M., & Almeida, J. (2021). Modelos descontínuos na análise tridimensional do comportamento hidromecânico de fundações de barragens de betão. *Geotecnia*, (151), 5-32. http://doi.org/10.24849/j.geot.2021.151.02.

Azevedo, N.M., Lemos, J., & Almeida, J. (2010). A discrete particle model for reinforced concrete fracture analysis. *Structural Engineering and Mechanics*, *36*(3), 343-361. http://doi.org/10.12989/sem.2010.36.3.343.

Azevedo, N.M., & Lemos, J. (2022). A hybrid particle/finite element model with surface roughness for stone masonry analysis. *Applied Mechanics*, *3*(2), 608-627. http://doi.org/10.3390/applmech3020036.

Dong, Z., Lin, T.R., Tang, S., Lang, Y., Yuan, R., & Heng, S. (2024). Mechanical properties and failure mechanism of concrete-granite composite specimens under compression load. *Construction & Building Materials*, *435*, 136768. http://doi.org/10.1016/j.conbuildmat.2024.136768.

Dong, W., Wu, Z., & Zhou, X. (2016). Fracture mechanisms of rock-concrete interface: experimental and numerical. *Journal of Engineering Mechanics*, *142*(7), 04016040. http://doi.org/10.1061/(ASCE)EM.1943-7889.0001099.

Enzell, J., Nordström, E., Sjölander, A., Ansell, A., & Malm, R. (2023). Physical model tests of concrete buttress dams with failure imposed by hydrostatic water pressure. *Water*, *15*(20), 3627. http://doi.org/10.3390/w15203627.

Farinha, M.L.B., Azevedo, N.M., & Candeias, M. (2017). Small displacement coupled analysis of concrete gravity dam foundations: static and dynamic conditions. *Rock Mechanics and Rock Engineering*, *50*(2), 439-464. http://doi.org/10.1007/s00603-016-1125-7.

Farinha, M.L.B., Azevedo, N.M., Leitão, N.S., Almeida, J.R., & Oliveira, S. (2022). Sliding stability assessment of concrete dams using a 3D discontinuum hydromechanical model following a discrete crack approach. *Geotechnics*, *2*(1), 133-157. http://doi.org/10.3390/geotechnics2010006.

He, J.N., Yang, D.W., & Zhenyu, W. (2022). System reliability analysis of foundation stability of gravity dams considering anisotropic seepage and multiple sliding surfaces. *Engineering Computations*, *39*(8), 3108-3128. http://doi.org/10.1108/EC-08-2021-0488.

Krounis, A., Johansson, F., & Larsson, S. (2015). Effects of spatial variation in cohesion over the concrete-rock interface on dam sliding stability. *Journal of Rock Mechanics and Geotechnical Engineering*, *7*(6), 659-667. http://doi.org/10.1016/j.jrmge.2015.08.005.

Li, X., Lan, L., Zhang, J., Tang, J., Lv, M., Liu, C., & Han, X. (2022). A new method for measuring the adhesion strength of rock-concrete specimens based on the calibration interface of the modified flat-joint model. *Engineering Failure Analysis*, *142*, 106752. http://doi.org/10.1016/j.engfailanal.2022.106752.

Li, Z.C. (2021). Global sensitivity analysis of the static performance of concrete gravity dam from the viewpoint of structural health monitoring. *Archives of Computational Methods in Engineering*, *28*(3), 1611-1646. http://doi.org/10.1007/s11831-020-09434-0.

Santos, V.O., Bressani, L.A., & Smirdele, C.S.D. (2023). Geotechnical behavior of gravity dams built on sedimentary rocks: pore pressures and deformations analysis of Dona Francisca HPP foundation. *Soils and Rocks*, *46*(2), e2023013622. http://doi.org/10.28927/SR.2023.013622.

Tian, H.M., Chen, W.Z., Yang, D.S., & Yang, J.P. (2015). Experimental and numerical analysis of the shear behaviour of cemented concrete–rock joints. *Rock Mechanics and Rock Engineering*, *48*(2), 213-222. http://doi.org/10.1007/s00603-014-0560-6.

Zhou, X.P., Fan, X.W., Du, E., Bi, J., & Berto, F. (2022). Hydromechanical coupling model for mechanical and hydraulic behavior of fractured rock mass in the framework of adanced general particle dynamics. *Fatigue & Fracture of Engineering Materials & Structures*, *45*(12), 3559-3576. http://doi.org/10.1111/ffe.13830.